Journal of Pharmacokinetics and Pharmacodynamics (2025) 52:17
https://doi.org/10.1007/s10928-025-09962-x

ORIGINAL PAPER

Defining preclinical efficacy with the DNAPK inhibitor AZD7648 in combination with olaparib: a minimal systems pharmacokinetic–pharmacodynamic model

Joost DeJongh[1] · Elaine Cadogan[2] · Michael Davies[3] · Antonio Ramos-Montoya[2] · Aaron Smith[3] · Tamara van Steeg[1] · Ryan Richards[4]

Received: 23 July 2024 / Accepted: 14 January 2025 / Published online: 17 February 2025

Abstract

AZD7648 is a potent inhibitor of DNA-dependent protein kinase (DNA-PK), which is part of the non-homologous end-joining DNA repair pathway. When combined with the PARP inhibitor olaparib, AZD7648 shows robust combination activity in pre-clinical ATM-knockout mouse xenograft models. To understand the combination activity of AZD7648 and olaparib, we developed a semi-mechanistic pharmacokinetic/pharmacodynamic (PK–PD) model that incorporates the mechanism of action for each drug which links to proliferating, quiescent, and dying cell states with an additional Allee effect-like term to account for the non-linear growth and regression observed at low cell densities. Model parameters were fitted to training data sets that contained continuous treatment of either monotherapy or the combination. The observed interaction of AZD7648 on olaparib PK was incorporated in the PK–PD model by an effect function specific for each of the drug's MoA and was found essential to quantify drug effects at high dose levels of combination treatments. The model was able to adequately describe the observed efficacy for both monotherapy and sustained regressions in combination groups, mainly driven by maintaining a > 2:1 AUC ratio of apoptotic:proliferating cell fractions. We found that this model was suitable for forecasting intermittent dosing schedules a priori and resulted in accurate predictions when compared to xenograft efficacy data, without the need for extra, descriptive terms to describe supra-additive effects under combined dose regimes. This model provides quantitative understanding on the combination effect of AZD7648 and olaparib and allows for the exploration of the full exposure landscape without the need to experimentally test all scenarios. Furthermore, the model can be utilized to assess what exposures would be necessary in the clinic by linking it to observed or predicted human PK exposures. The model suggests 64.9 uM olaparib is sufficient to achieve tumor stasis in the absence of AZD7648, while the combination of AZD7648 and olaparib only requires plasma concentrations of 20.2 uM AZD7648 and 19.9 uM olaparib at steady-state to achieve the same effect.

Keywords Preclinical · Onoclogy · Population PKPD model · Tumor growth inhibition · Combination · Allee effect

Introduction

Many standard-of-care and novel oncology drugs are designed to affect DNA replication, where the mechanisms of the DNA damage response (DDR) and the cell cycle are well studied [1, 2]. One such compound, AZD7648, is a novel, potent and selective inhibitor of DNA-dependent protein kinase (DNA-PK) which is a key component of the non-homologous end-joining repair (NHEJ) pathway. AZD7648 has been shown to act as an effective sensitizer when combined with irradiation- or doxorubicin-induced DNA damage, leading to robust efficacy in preclinical models [3]. Additionally, it was found that treatment of AZD7648 in ATM-deficient models resulted in tumor regressions when combined with the PARP inhibitor olaparib, which is an approved treatment in breast, ovarian, pancreatic, and prostate indications [4–7]. ATM-deficient cells show an imbalance between homologous recombination repair (HRR) and NHEJ repair of broken replication forks caused by olaparib,

✉ Ryan Richards
Ryan.Richards@astrazeneca.com

[1] LAP&P Consultants BV, Leiden, The Netherlands

[2] Bioscience, Early Oncology R&D, AstraZeneca, Cambridge, UK

[3] DMPK, Early Oncology R&D, AstraZeneca, Cambridge, UK

[4] DMPK, Early Oncology R&D, AstraZeneca, Waltham, MA, USA

which results in chromosomal aberrations leading to cell death [8, 9]. Though it is unclear how ATM regulates the decision point between HR and NHEJ, increased chromosomal aberrations were observed for the combination when compared to either single agent.

Quantification of observed drug effects reported from pre-clinical in vivo studies often does not provide enough resolution for selection of optimal drug combinations, dose levels and the scheduling of active/recovery cycles [10]. PK–PD modelling, accounting for the underlying mechanisms of action of specific compounds, will likely improve the quantitative understanding of the observed efficacy on preclinical xenograft growth and regression. As such, these insights will improve the path to further drug development stages. This is especially important for drug combinations in order to quantitatively understand the biological interaction and exposure space required to achieve maximal efficacy within the therapeutic bandwidth.

The current analysis was performed to explain and predict effects on xenograft tumours from a bespoke ATM knock-out cell line (FaDu), during and after monotherapy or various combination treatment regimens with olaparib and AZD7648, to define requirements for pre-clinical efficacy. The main objective was to investigate whether this could be captured quantitatively based on the biological pathways underlying these compounds without the need for introducing additional empirical terms to capture apparent synergies between treatment effects under combined exposure.

To this end, a population PK–PD analysis for effects of DNA damage (olaparib) and inhibited DNA damage repair (AZD7648) on xenograft growth dynamics was developed using a multi-compartment minimal systems model fitted to data reported from an ATM-deficient mouse xenograft model. Several semi-mechanistic PK–PD-efficacy combination models exist in the literature that successfully capture tumor growth dynamics by incorporating varying degrees of mechanistic biomarker data [11–13]. The approach described here utilized a minimal semi-mechanistic model which introduced an additional Allee effect-like term that accounts for sustained regressions observed in some combination groups. Compound-specific effects were driven by respective plasma drug levels obtained from PK analysis in satellite animal groups. Exposure of AZD7648 and olaparib acting on the dynamic equilibrium between proliferative, quiescent, and apoptotic xenograft cell states was used to describe and explain quantitative and qualitative differences between various continuous 28-day combination treatments. From the same model parameters, treatment effects from drug combinations over a range of 42-day intermittent active/recovery cycles, were adequately described. Thus, a semi-mechanistic model which was fully identifiable was built to describe and forecast relevant aspects of combination activity in the xenograft model with adequate precision. Such a model aids in drug development to describe the windows of optimal exposure space/schedules required to maintain efficacy under a variety of treatment regimens within the therapeutic window.

Materials and methods

Ethics statement

Murine studies in the UK were conducted in accordance with UK Home Office legislation, the Animal Scientific Procedures Act 1986, the AstraZeneca Global Bioethics policy or Institutional Animal Care and Use Committee guidelines. Experimental work is outlined in project license PP3292652.

Pharmacokinetic and tumour xenograft studies

Plasma concentration data obtained after single or multiple intravenous and oral dosage of AZD7648 and/or olaparib to SCID and Nude mice were obtained from a total of eight studies. Details on the design, execution and analysis of these PK study data have been reported before [3] (Fok et al.). Briefly, Immunocompromised SCID (C.B-17/IcrHan®Hsd-Prkdcscid) or Hsd:Athymic Nude-Foxn1nu female mice (Envigo) were used for PK studies of AZD7648 and Olaparib. Blood samples were taken via venipuncture of the tail vein. 20 ul whole blood was taken per time point and mixed 1:5 with PBS and centrifuged at 1500g for 3 min at 4 °C, and the plasma was extracted and frozen at − 80°C. In total a maximum of 100ul whole blood was taken over a 24 h period.

Each plasma sample was prepared using an appropriate dilution factor, and compared against an 11 point standard calibration curve (1–10,000 nM) prepared in DMSO and spiked into blank plasma. Protein precipitation was carried out by the addition of 4 volumes of ice cold acetonitrile containing the internal standard followed by shaking for 10 min and centrifugation at 3000 rpm for 10 min. Supernatant was then diluted in six volumes of water and analyzed via UPLC-MS/MS. Performance criteria used were % CV values of ± 25% and an LLOQ of 0.009nM for both olaparib and AZD7648. Data on xenograft growth, inhibition and regression were obtained from four in vivo studies. Xenograft studies using the FaDu ATM KO model was established by implantation of 100 µL of a cell suspension subcutaneously into the dorsal left flank of female severe combined immunodeficient (SCID) (C.B-17/IcrHan®Hsd-Prkdcscid) mice of at least 6 weeks of age. Tumours were measured (length x width) by bilateral Vernier calliper measurements and tumour volume calculated using Mousetrap software. Mice were randomized into treatment groups when mean tumour volume reached ~ 0.2 cm^3. AZD7648

was formulated in 0.5% hydroxypropyl methylcellulose (HPMC)/0.1% Tween80 (HPMC/T) and orally dosed. Olaparib was formulated in 10% DMSO/30% Kleptose and orally dosed at 100 mg/kg once daily. Olaparib was dosed 1 h after the morning dose of AZD7648 or its vehicle HPMC/T in all combination studies. Tumour growth inhibition from start of treatment was assessed by comparison of the mean change in tumour volume for the control and treated groups, using the Mousetrap application and represented as tumour growth inhibition (TGI).

Computation and model development

The population PK and PK–PD analysis was performed by means of non-linear mixed-effects modelling as implemented in the NONMEM software package (version 7 level 4.3; Icon Development Solutions, Ellicott City, Maryland, USA) in combination with PsN (version 4.7.0). Gfortran (version 4.6.0) was used as compiler. Diagnostic graphics, exploratory analyses, and post-processing of NONMEM output were performed using R (version 3.4.4, The R foundation for Statistical Computing) and Rstudio (version 1.1.463, Rstudio Inc, Boston, USA) used in conjunction with a custom-built modelling interface. Calculations and computations were run on an Intel CITM i7-7700 CPU @ 3.60 GHz. Differential equations were solved numerically in NONMEM using ADVAN6 or 13. The first-order conditional estimation method with interaction (FOCEI) was used for parameters estimation [14, 15].

Population PK and PK–PD analyses are based on the assumption that treatment effects in living organisms are dependent on the drug concentration which changes over time after a dose is given. These changes can be captured as a function of time and exposure by a combination of fixed effect parameters (e.g. clearance and distribution volume) and two levels of random effect parameters: one for biological variability between individual subjects (intra-individual variability, IIV) and one level of variability within each subject, due to e.g. measurement errors, model misspecification and other sources of residual variability. Random effects for inter-individual variability were described using exponential terms reflecting log-normal distributions of model parameters. Residual variability was explored with a proportional error model on PK and PD observations [16, 17]. Goodness of model Fit to the data (GoF) was evaluated continuously during PK and PK model development by various diagnostic metrics [18, 19].

PK model A 2-compartment model with 1st order absorption and a mixed linear/non-linear clearance was used to describe AZD7648 pharmacokinetics

$$\frac{dA1}{dt} = K_a \cdot A_g - Q \cdot \frac{A1}{V_c} + Q \cdot \frac{A2}{V_p} - \left(Cl \cdot \frac{A1}{V_c} + \left(\frac{Vmax}{\frac{A1}{V_c} + Km} \right) \right) \quad (1)$$

$$\frac{dA2}{dt} = Q \cdot \frac{A1}{V_c} - Q \cdot \frac{A2}{V_p} \quad (2)$$

$$C_{p,AZ} = \frac{A1}{V_c} \quad (3)$$

where K_a is the absorption rate, A_g is the amount of drug in gut (µmol), Q is the intercompartmental clearance, A1 is the quantity of AZD7648 in the central compartment (µmol), A2 is the quantity of AZD7648 in the peripheral compartment (µmol), $C_{p,AZ}$ is the concentration of AZD7648 in plasma, V_c and V_p are the volumes of distribution in the central and peripheral compartments, Cl is the linear clearance, Vmax is the maximal elimination rate and Km is the concentration at half maximal elimination.

Similarly, olaparib was described by a 2 compartment model with 1st order oral absorption and linear clearance. An additional interaction term was included to account for the observed drop in clearance when in combination with AZD7648:

$$\frac{dA3}{dt} = K_a \cdot A_g - Q \cdot \frac{A3}{V_c} + Q \cdot \frac{A4}{V_p} - \left(Cl \cdot \frac{A3}{Vc} \right) \cdot CmS \quad (4)$$

$$\frac{dA4}{dt} = Q \cdot \frac{A3}{V_c} - Q \cdot \frac{A4}{V_p} \quad (5)$$

$$C_{p,olap} = \frac{A3}{V_c} \quad (6)$$

$$Cms = 1 \quad if \;\; Dose_{AZ} = 0 \quad (7)$$

$$Cms = 1 - \frac{Dose_{AZ}}{Dose_{AZ} + CmD50} \quad if \;\; Dose_{AZ} > 0 \quad (8)$$

where A3 is the amount of olaparib in the central compartment (µmol), A4 is the amount of olaparib in the peripheral compartment (µmol), $C_{p,olap}$ is the concentration of olaparib in plasma, Cms is the combination interaction term, $Dose_{AZ}$ is the dose of AZD7648 (mg/kg/day) and CmD50 is the daily dose of AZD7648 that reduces clearance by 50%. All parameter values are listed in Tables 1 and 2 and the model code is provided in the supplementary materials.

Tumor PK–PD model Tumor volume was described by a proliferating cell compartment (Prol), quiescent cell compartment (Quiesc), and two dying cell compartments (ApopI/II). Untreated tumor cells undergo logistic growth

Table 1 Parameters of the population PK model for AZD7648 in SCID and nude mice

Parameter	Abbreviation	Units	Value	SE	95% Conf. interval		RSE (%)
Fixed effects							
Abs. rate constant	Ka*	(h^{-1})	2.77	0.217	2.35	3.20	7.83
Clearance	CL	(L/kg/h)	0.251	0.0193	0.213	0.289	7.69
Max. Elim. Rate	Vmax	(umol/kg/h)	4.27	0.562	3.17	5.38	13.1
Conc. at haf max.elim	Km	(uM)	3.73	0.310	3.12	4.33	8.32
Central distrib vol	V_c	(L/kg)	3.45	0.594	2.28	4.61	17.2
Peripheral. distrib vol	V_p	(L/kg)	Assumption: $V_p = V_p$				
Intercomp. clearance	Q	(L/kg/h)	0.932	0.219	0.503	1.36	23.5
Random effects for inter-individual variability							
Om_1 (CL + Vmax)			0.0631	0.0116	0.0403	0.0858	18.4
Om_1 × 2			− 0.0291	0.0350	− 0.0977	0.0395	− 120
Om_2 (V)			0.193	0.0554	0.0848	0.302	28.6
Proportional Residual Error (variance)			0.304	0.0290	0.247	0.361	9.52
F1 (relative to SCID mice)*			− 0.520	0.183	− 0.880	− 0.160	− 35.3
Ka (h^{-1})*			9.90 (fixed, due to lack of informative samples)				
Condition number: 243							

*Strain identified as categorical covariate for Nude mice on two PK parameters

Table 2 Parameters of the population PK model for olaparib in SCID and Nude mice

Parameter	Abbreviation	Units	Value	SE	95% Conf. interval		RSE (%)
Fixed effects							
Absolute bio-avail	F1		0.598	0.0927	0.416	0.779	15.5
Abs. rate constant	Ka	(h^{-1})	10.0 (fixed by assumption, due to lack of data)				
Clearance	CL	(L/h)	1.95	0.226	1.50	2.39	11.6
Central distrib. vol	V_c	(L/kg)	1.17	0.192	0.789	1.54	16.5
Intercomp. clearance	Q	(L/h)	0.668	0.0857	0.500	0.836	12.8
Peripheral distrib. Vol.	V_p	(L/kg)	2.66	0.353	1.97	3.35	13.3
AZD7648 daily dose corresponding to a − 50% change in CL for olaparib		(mg/kg/day)	82.5	16.2	50.7	114	19.7
Random effect for inter-individual variability							
Om_1 (V_c)			0.591	0.141	0.314	0.869	23.9
Proportional residual error (variance)			0.399	0.0646	0.273	0.526	16.2
F1 11,448 (Nude)*			0.425	0.0644	0.299	0.552	15.1
F1 1734 (Nude)*			0.238	0.0409	0.158	0.318	17.1
F1 1143 (Nude)*			0.174	0.0439	0.0884	0.261	25.2
F1 1721 (Nude)*			0.489	0.0788	0.334	0.643	16.1
F1 1770 (SCID)*			1.48	0.323	0.845	2.11	21.9
F1 1816 (SCID)*			4.18	1.54	1.17	7.20	36.8
Condition number: 271.1							

*Strain and study number identified as categorical covariates for absolute bio-availability

described by the growth rate (GC) and carrying capacity (KC). Treatment with olaparib causes proliferating cells to enter a reversible DNA-damage induced quiescent state, where cells can irreversibly transition to damaged states before dying. Quiescent cells undergo DNA repair through NHEJ, which can be inhibited by AZD7648:

$$TX_{eno} = Prol + Quiesc + ApopI + ApopII \tag{9}$$

$$\frac{dProl}{dt} = Prol \cdot GC \cdot \left[1 - \left(1 - \frac{K_{to}}{2}\right) \cdot \frac{TX_{eno}}{KC}\right] \cdot AlleeEff - OlEff \cdot K_{to} \cdot Prol + AzEff \cdot K_{to} \cdot Quiesc \tag{10}$$

$$\text{Prol}(0) = \text{BL}$$

$$\frac{dQuiesc}{dt} = -K_{to} \cdot Quiesc + OlEff \cdot K_{to} \cdot Prol - AzEff \cdot K_{to} \cdot Quiesc \tag{11}$$

$$\text{Quiesc}(0) = 0$$

$$\frac{dApopI}{dt} = K_{to} \cdot Quiesc - ApopI \cdot K_{to} \quad \text{ApopI}(0) = 0 \tag{12}$$

$$\frac{dApopII}{dt} = K_{to} \cdot ApopI - ApopII \cdot K_{to} \quad \text{ApopII}(0) = 0 \tag{13}$$

where TX_{eno} is the total tumor volume, BL is the initial tumor volume, K_{to} is the turnover rate constant for various transitions, GC is the tumor growth rate, and KC is the carrying capacity. The effects of olaparib (OlEff) and AZD7648 (AZEff) on tumor cells were described using biophase concentrations $C_{e,Olap}$ and C_{eAZ} to account for the delay between pharmacokinetics and pharmacological effect. The olaparib effect was best described by a linear function, while AZD7648 was best described by a sigmoidal function:

$$\frac{dC_{e,Olap}}{dt} = K_{tr} \cdot \left(C_{p,Olap} - C_{e,Olap}\right) \tag{14}$$

$$\frac{dC_{e,AZ}}{dt} = K_{tr} \cdot \left(C_{p,AZ} - C_{e,AZ}\right) \tag{15}$$

$$OlEff = C_{e,Olap} \cdot EC_{olap} \tag{16}$$

$$AzEff = 1 - \frac{C_{e,AZ}}{C_{e,AZ} + EC50_{AZ}} \tag{17}$$

where $C_{e,Olap}$ and $C_{e,AZ}$ are the effective concentrations of olaparib and AZD7648 in the biophase compartment, $C_{p,Olap}$ and $C_{p,AZ}$ are the plasma concentrations of olaparib and AZD7648, K_{tr} is the transit rate constant for biophase distribution, EC_{olap} is the linear effect coefficient for olaparib, and $EC50_{AZ}$ is the concentration to illicit 50% inhibition of transition from Quiesc to Prol.

Additionally, an Allee effect term was added to the proliferating compartment to account for non-linear growth and regressions, which was described by sigmoidal function

$$AlleeEff = \frac{Prol^G}{Prol^G + AEc^G} \tag{18}$$

where AEc is the proliferative cell mass that corresponds to 50% effect and G is the slope.

PK analysis for AZD7648 and/or olaparib in mice

Plasma concentration data after single or multiple oral dosage of AZD7648 and olaparib as mono- or combination therapy in SCID and nude mice were pooled in a single comprehensive dataset to allow for population PK analysis according to NONMEM required data formatting. In the PK analysis, the data were subjected to compartmental PK analyses, with two-compartment distribution, first order absorption from a dose compartment with linear and/or Michaelis–Menten elimination from the central compartment.

PK–PD analysis for tumour growth inhibition (TGI)

Xenograft growth data over time were collected from two studies in (SCID) mice that were combined in a single PK–PD dataset and assigned to model-calibration and validation subsets (Table S1). Unperturbed xenograft growth was analysed by fitting the logistic Verhulst model to xenograft data from vehicle-treated control animals.

The calibration dataset for PK–PD model development consisted of xenograft data from one study in which eight animal groups received either active treatment QID with 50–100 mg/kg AZD7648 and/or 50–100 mg/kg olaparib for a period of 4 weeks, followed by a wash-out phase of up to eight weeks (Fig. S3). Control groups were treated with vehicle continuously for 4 weeks.

The validation subset consisted of a mouse study, in which eight groups of animals were treated during six weeks according to various dose schedules, partially following subsequent active treatment/recovery phases, summarized in Table S1 with raw results visualized in Fig. S6.

Xenograft growth and turn-over was postulated based on the family of indirect response models [20], according to various papers from the literature on pre-clinical oncology models [10, 21] and a priori knowledge on the mechanism of action for both compounds.

The primary xenograft cell state was described by two compartments represent either proliferative or apoptotic cell states. Transit compartments were applied for delay between apoptosis and cell death resulting in loss of xenograft volume. Olaparib stimulates cell transition from a proliferative to an apoptotic state and AZD7648 acts by inhibiting transition of cells from an apoptotic to a proliferative state. System- and drug-specific model parameters were iteratively optimised by simultaneous fitting of model parameters to all eight treatment groups in S1822. The model structure was expanded and refined by learning from the data through population-based model development, based on forward addition/backward deletion of fixed and random effects with diagnostic analyses of the residuals between observations and model-predictions [18].

During the entire model development process, various assumptions on rate constants for xenograft cell dynamics were tested to identify rate-limiting steps and reduce parameter space when necessary and if possible.

For optimal system and drug-specific parameter identification, PK–PD model development was performed by sequential and simultaneous fitting to data from control, single and combination treatment groups reported in study S1822, which served as the main model calibration dataset.

Model evaluation

Goodness-of-fit was determined using the minimum value of the objective function (MVOF) defined as minus twice the log-likelihood. For nested models, a decrease of 10.8 points in the MVOF (corresponding to $p < 0.001$ in a chi-squared distribution) after adding an additional parameter was considered significant. The goodness-of-fit was also investigated by visual inspection of the plots of individual predictions and the diagnostic plots of (weighted) residuals. In addition, visual predictive checks (VPC) were performed in which the median and the 95% prediction interval of data simulated with the developed model ($N = 200$) were plotted together with the observations [18].

Results

Population PK model analysis of AZD7648 and olaparib in mice

PK data from both SCID and Nude mice strains were pooled together to create population PK models for AZD7648 and olaparib (Figs. 1 and S1). For both compounds, the PK model structures were based on two-compartment distribution with first-order oral uptake and elimination from the central compartment. Random effects for inter-individual variability between animals were included in the models. Observed differences in absorption rate and bioavailability were captured using separate parameters between strains.

AZD7648 was described by a reduced two-compartment model ($V_c = V_p$) with terms for both linear and non-linear elimination. Absorption was modelled by a first-order rate constant K_a, estimated by fitting to the results from the SCID mice strain. For Nude mice, K_a needed to remain fixed to a high value of 9.9 h^{-1}, validated by likelihood profiling, due to the absence of data in the absorption phase. Relative bioavailability of AZD7648 in Nude mice was found to be lower compared to the SCID strain and was accounted for by fitting a dedicated parameter for relative F1 in this strain. Random effects for inter-individual variability were identified on V_c and on the sum of both elimination routes. A non-diagonal element was included in the Omega matrix to account for their correlation.

All parameters could be identified with adequate precision (Table 1) and the VPC's illustrate the goodness of fit of the final PK model for AZD7648 from the most informative study after single dosage in SCID mice (Fig. 1a) and in combination with Olaparib (Fig. 1b). For multiple dose data the PK was also adequately captured by this model (Fig. S1). Olaparib PK data from various studies in mice was described by a two-compartment model with a single, linear term for elimination. A first-order rate constant Ka was fixed to a high value (10 h-1) for oral absorption, as no informative data during the immediate post-dosage phase were available.

Co-treatment with AZD7648 was found to increase olaparib exposure. This was implemented in the PK model by a dedicated drug-drug interaction parameter for a decreased olaparib clearance as a function of the daily AZD7648 dose (Table 2). The degree of interaction of AZD7648 on olaparib concentrations during multiple dosing becomes apparent by removing the interaction term from the PK model (Fig. S2). Absolute olaparib bio-availability after oral dosage was based on a study with arms for both i.v. and for p.o. dosage. Relative oral bioavailability was found to vary substantially between some studies, even within the same mice strain, and was accounted for in the final PK model by fitting a descriptive inter-study scaling factor on this parameter. A single random effect for inter-individual variability for olaparib PK was included for the central distribution volume Vc. All PK parameters for olaparib showed adequate precision (Table 2) and the resulting model fit was able to describe single and multiple dose data for olaparib dosed alone (Fig. 1c) or combined with AZD7648 (Fig. 1d). For both compounds, the estimated values for PK model parameters were carried over to the PK–PD analysis. Imputation of the population PK parameters values into the PK–PD

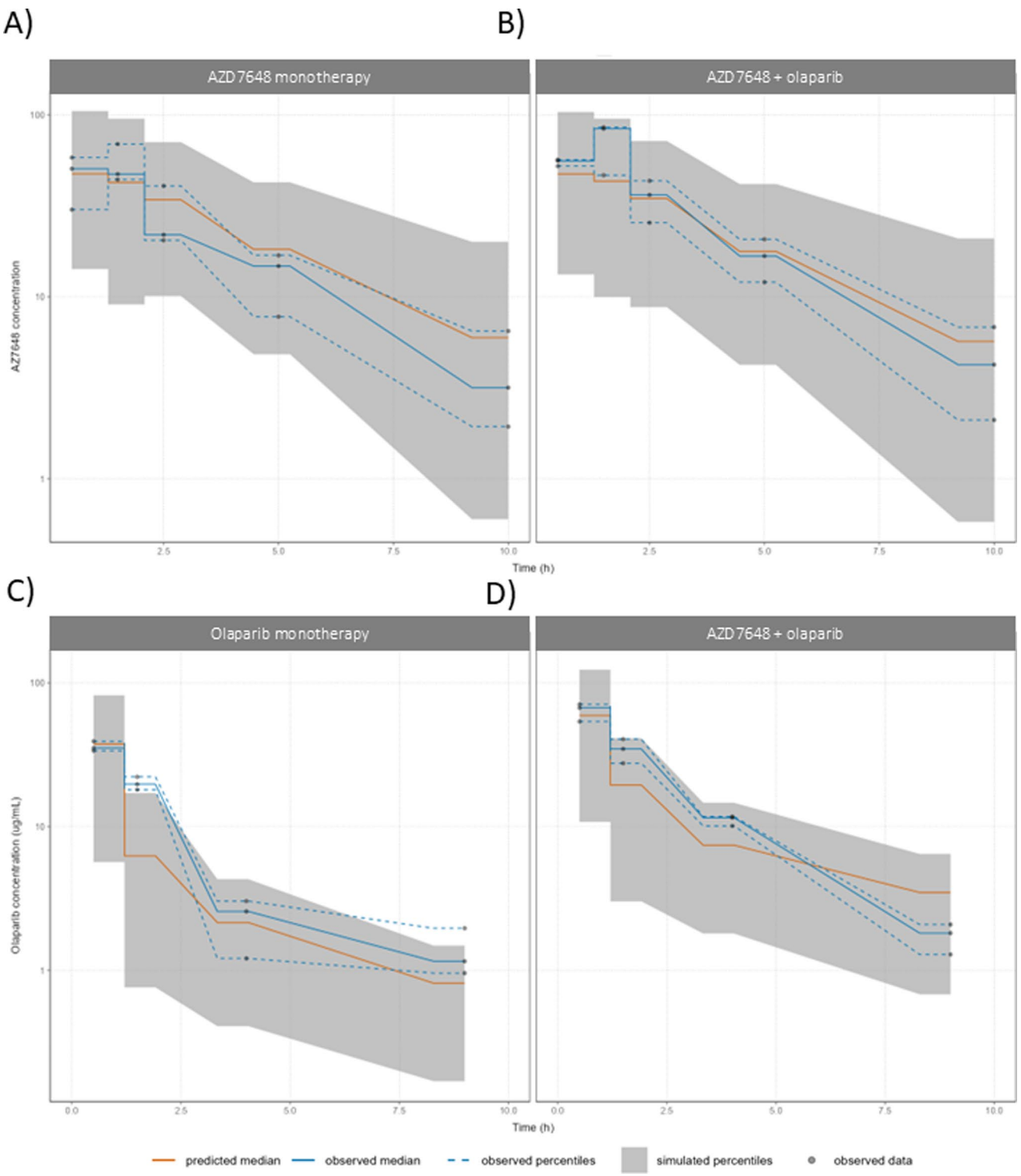

Fig. 1 VPC's for population PK models of AZD7648 and olaparib as mono- or combination therapy after single dosing in SCID mice. **a** 100 mg/kg AZD7648 as monotherapy after a single dose. **b** 100 mg/kg AZD7648 combined with 100 mg/kg olaparib after a single dose. **c** 100 mg/kg olaparib as monotherapy after a single dose. **d** 100 mg/kg olaparib combined with 100 mg/kg AZD7648 after a single dose. Shaded regions are 10–90% prediction intervals. Open symbols are observed PK from 3 mice for monotherapy (black) or the combination (red). Dashed lines represent the 10–90% observed percentiles (Color figure online)

model allowed modelling of xenograft growth and regression dynamics as a function of typical drug plasma concentrations. As most PK data was obtained from satellite groups, only fixed effects from the population PK models for olaparib and AZD7648 were taken forward.

Xenograft growth and regression observed under single and combination treatment regimens

Xenograft tumor volume data were obtained from S1822, in which animals were dosed continuously for 28 days with either vehicle, AZD7648 or olaparib monotherapy, or five combination regimes at various dose levels (Fig. 2a; Table S1). Growth and regression during and after treatment

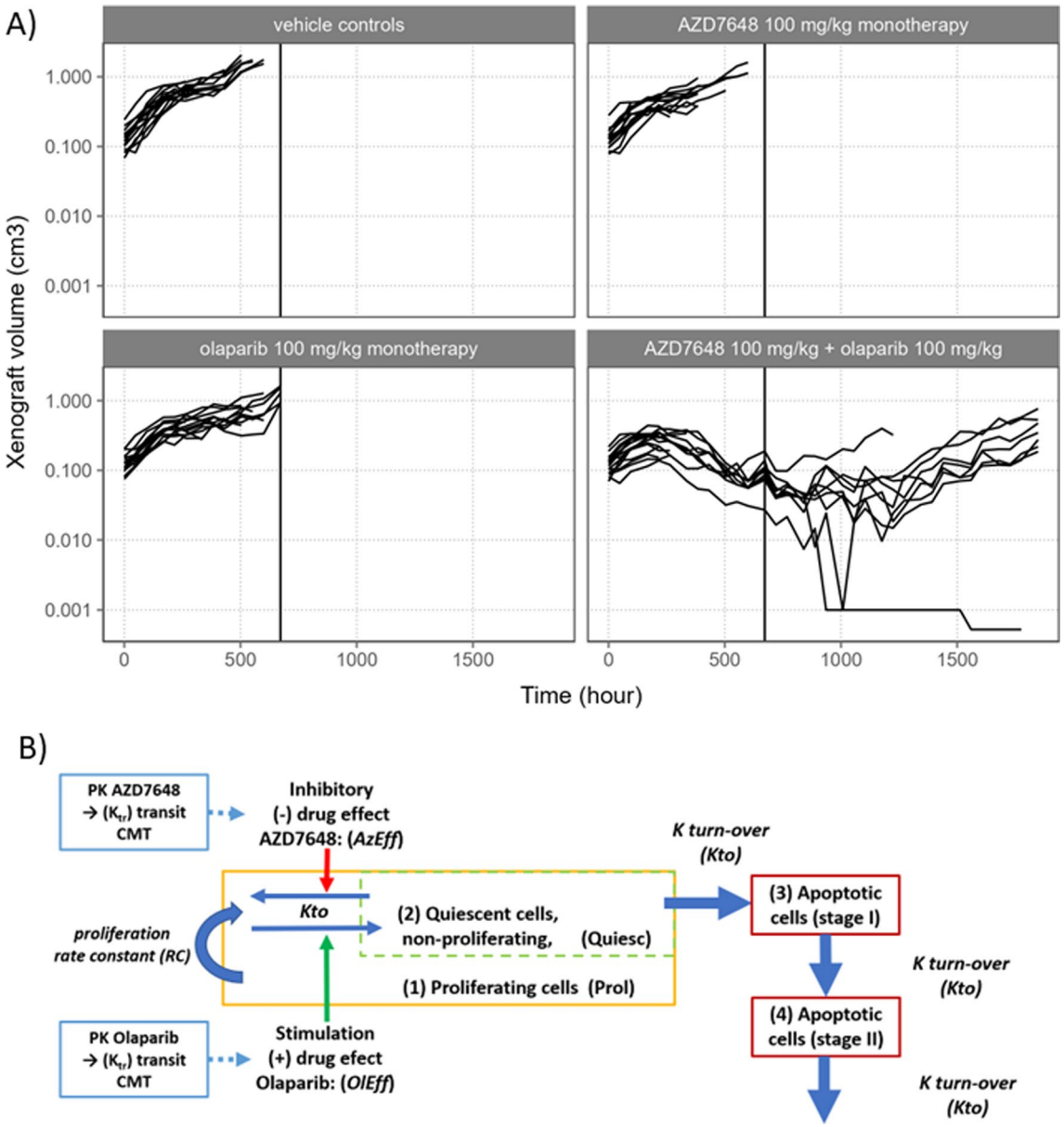

Fig. 2 Observed tumor growth inhibition in individual ATM-knockout mice and the hypothesized xenograft model structure. **a** Individual tumor volumes from treatment with vehicle (black), 100 mg/kg AZD7648, 100 mg/kg Olaparib, and 100 mg/kg AZD7648 + 100 mg/kg Olaparib. Vertical lines represent the end of treatment. Compounds were dosed orally once daily for 28 days. **b** PK–PD model structure to capture the combination effect of AZD7648 and Olaparib. Cells proliferate with a rate constant RC. Treatment with Olaparib facilitates the DNA damage response and conversion to a non-proliferating state (NPROL) at rate constant K_{to}. Non-proliferating cells can recover or enter the apoptotic pathway non-reversibly by rate constant K_{to}. AZD7648 prevents the recovery of non-proliferating cells by inhibiting the DNA repair process

show the qualitative requirements for a PK–PD model to describe and explain these data (Fig. 2b).

Vehicle-treated control animals showed self-limiting tumor growth that initially started as exponential growth, decreasing as the tumor approaches a maximum sustainable volume (carrying-capacity). This carrying capacity represents the xenograft's upper equilibrium state, where cell proliferation equals cell death. Both inter- and intra-individual variability appear from the observations (Fig. S3). Treatment with either 100 mg/kg/day AZD7648 or 100 mg/kg/day olaparib inhibited tumor growth relative to the control animals, but never resulted in regression below base-line volumes. In contrast, combined exposure at these dose levels resulted in regression below the pre-treatment volume. After the 28 days of treatment in the combination group, delayed tumor re-growth was observed, except for one animal showing sustained post-treatment regression. Similar tumor responses to four additional combination treatments were observed in the same study (Fig. S3).

Description of these qualitative and quantitative differences between various treatment groups, including delayed response to, and recovery from, active treatment, required a multi-compartment PD model structure (Fig. 2b). Based on the specific transition between cell states driven by olaparib and AZD7648 exposure, a minimal model for tumor growth over time represents the following cell states: (1) A pool of proliferating cells that divide according to a logistic (Verhulst) growth equation; (2) A pool of quiescent cells that remain in a temporary state of stasis. The cells from this pool may transit either back to a proliferative state, or they may reach state (3), representing the irreversible state of cell death that eventually results in removal from the tumor with corresponding volume loss. Similar models on pre-clinical PD of various cytotoxic and cytostatic compounds, with a series of transit compartments to describe the cell death process, have been reported previously [22–24].

Development, optimization and evaluation of the population PK–PD model

During the first step, a logistic (Verhulst) model for unperturbed tumor growth in mice was fitted to quantify the baseline volume as a boundary condition specific for each individual animal. Parameters for the final PK–PD model, including unperturbed growth (GC) and carrying capacity (KC) were fit simultaneously to all treatment groups. This model fit was accurate and precise as appeared from the parameter table and VPC's for control groups of each study (Table 3, Fig. S4). A second step was performed by iterative model optimization, using xenograft growth data reported from a single study where animals were dosed continuously

Table 3 Model parameters for xenograft growth, inhibition, shrinkage, and remission in olaparib and/or AZD7648-treated mice groups in study 1/S1822

Parameter	Abbreviation	Units	Value	SE	95% Conf. interval[a]	RSE (%)[b]
Structural, Θ						
Xenograft volume at baseline	BL	(cm^3)	0.115	0.00449	(0.106, 0.124)	3.9
Growth rate coefficient S1822	GC	(day^{-1})	0.329	0.0184	(0.293, 0.365)	5.6
Carrying capacity	KC	(cm^3)	2.25	0.130	(1.99, 2.50)	5.8
Allee effect size at 50%	AEC	(mm^3)	1.93	0.222	(1.50, 2.37)	11
Power coefficient on Allee effect	G	–	0.637	0.0598	(0.520, 0.754)	9.4
Effect transit rate constant	K_{tr}	(day^{-1})	0.961	0.166	(0.637, 1.29)	17
EC50 of AZD7648	$EC50_{az}$	(uM)	8.99	0.667	(7.68, 10.3)	7.4
Olaparib linear effect coefficient	EC_{olap}	(uM^{-1})	0.0154	6.96×10^{-4}	(0.0141, 0.0168)	4.5
Kturn-over[c]	K_{to}	(day^{-1})				
Proportional residual error			0.243	0.00485	(0.233, 0.252)	2.0
Inter-individual variability, Ω						
ω^2 Om_1 (BL)			0.0951	0.0142	(0.0674, 0.123)	15
ω_{xy} Om_1 (BL)×Om_2(AEC)			0.135	0.0607	(0.0164, 0.254)	45
ω^2 Om_2 (AEC)			1.83	0.411	(1.03, 2.64)	22
ω^2 Om_3 (GC)			0.0362	0.00797	(0.0206, 0.0518)	22
Condition number: 40.12						

[a]Interval for parameter u calculated as $\hat{u} \pm \Phi(1-\alpha/2)\times se(\hat{u})$

[b]RSE (%) for parameter u calculated as $|100\times se(\hat{u})/\hat{u}|$

[c]Kturn-over was assumed to be equal to the Growth rate Coefficient GC, as these parameters could not be identified independently from the model fit to the data

with AZD7648, olaparib, or the combination. This served as the model calibration dataset.

The positive effect of olaparib on cell transition, from a proliferating (1) to a quiescent (2) state, was modelled as a single drug effect parameter with a positive, linear dependence on plasma concentration (OlEff). The inhibiting effect of AZD7648 on transition from the quiescent to the proliferating cell state, was modelled by a saturable function, with a potency (EC50) fitted and a maximum drug effect (Emax) fixed to − 1, corresponding to complete inhibition. For both compounds, a delay between plasma drug concentrations and actual effects in xenograft cells on these transition processes was modelled by a transit compartment model with a fitted rate constant (K_{tr}). Turn-over/cell death of apoptotic (3) xenograft cells from the quiescent pool was modelled as a one-directional process with a first-order rate constant for transit through two compartments (3 & 4) before final cell death and removal from the xenograft. Alternative transit models with one or three compartments were also considered, but based on various GoF criteria, two compartments were found optimal for describing delayed cell death in the currently analysed studies. The final xenograft PD model consisted of four differential equations for xenograft cell mass (Fig. 2b).

The core PK–PD model structure outlined above was able to describe xenograft growth inhibition observed with monotherapy treatment during 28 days of continuous treatment (Fig. 3a). For combination treatment, delayed xenograft regression was observed. Most animals in this group had tumor regrowth occur post-treatment, with one animal

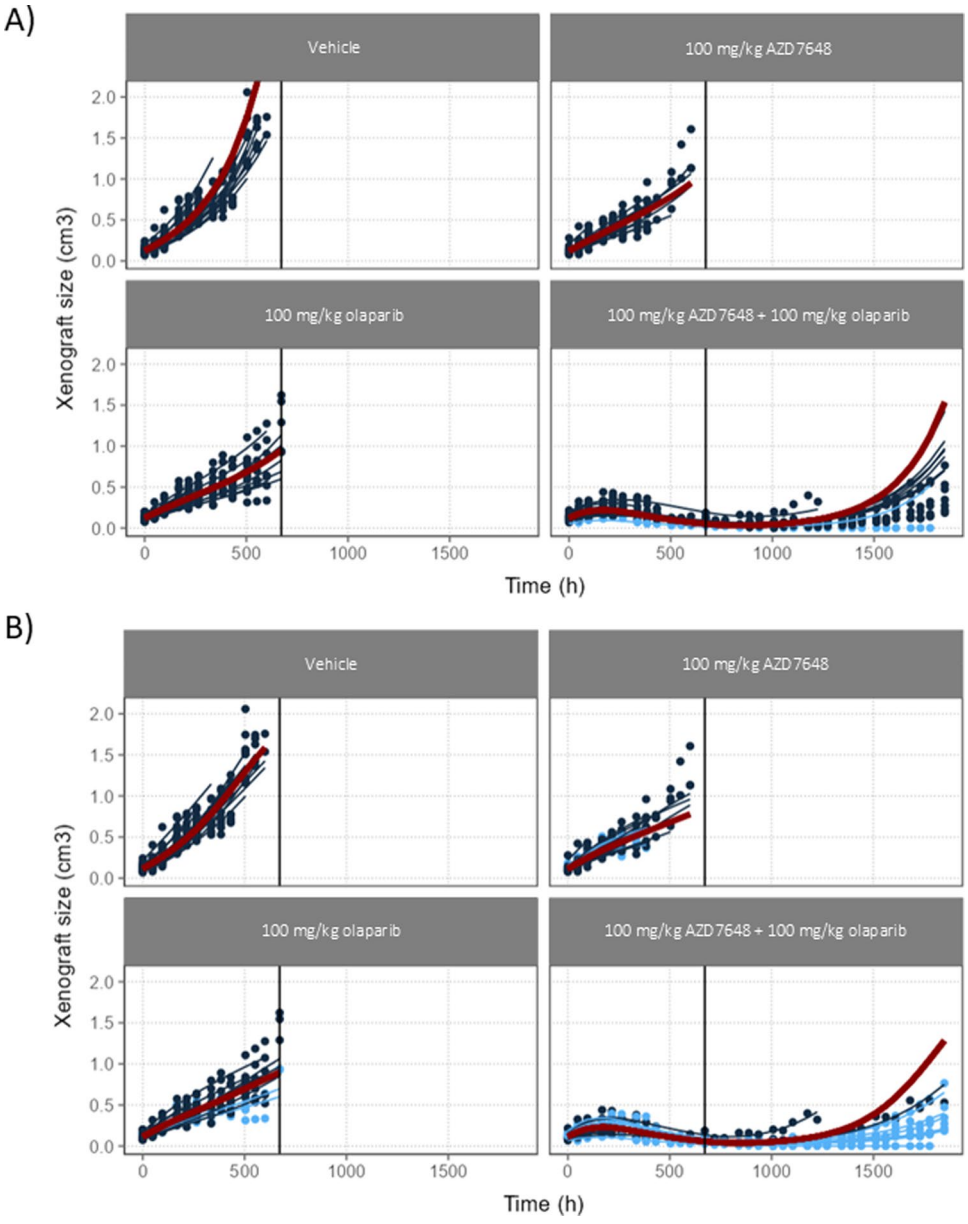

Fig. 3 Observed and model-fitted curves for the xenograft PK–PD model with and without Allee effect after treatment with AZD7648, Olaparib, or the combination. **a** Results of the PK–PD model using only continuous logistic growth and drug mechanism-driven tumor regression. **b** Results of PK–PD with the inclusion of the Allee effect term expressed at low cell densities with probability for permanent tumor regression. circles—observed tumor volumes in individual mice; lines—individual fits (IPRED); red lines—population median fits (PRED); Blue circles and lines mark individual high responders to treatment, based on Eta's. Vertical reference line—end of four-week active exposure (Color figure online)

that showed sustained regression after the end of active treatment. The latter phenomenon also occurred in combination groups from a separate study (S1842), in which various continuous and intermittent dose combinations were studied (Table S1). The initial PD model fit resulted in post-treatment re-growth predictions for all animals with a biased prediction of the median xenograft volume and inability to adequately fit data from individual animals in the combination treatment group (Fig. 3a).

To achieve adequate description of permanent xenograft regression observed in combination groups, an additional term was added to the growth coefficient for the proliferative state. This was implemented as an inhibition term which could vary between unity (no effect) and zero (max. effect) and was based on the Allee effect [25–29]. The additional term allowed description and prediction of sustained xenograft regression after treatment when proliferating cell levels were low, as was observed in individual mice under combination treatment at high dose levels (Fig. 3a). This plot demonstrates a clearly visible improvement over the initial model (Fig. 3b). The Allee effect can lead to three different equilibrium states of normal tumor growth (no Allee effect), stable disease (moderate Allee effect), or sustained regression (strong Allee effect) (Fig. S5). The two associated PD model parameters estimated for this show adequate precision (Table 3). Comparison between fit plots obtained before and after implementation of this model term demonstrate the qualitative and quantitative improvement on the description of xenograft regression in combination treatment. For all other animals under combination treatment, median xenograft growth inhibition/regression was adequately described during and after treatment (Figs. S6 and S7).

Optimal random effect parameter assignment of inter-individual variability (IIV) was explored from standard diagnostic plots and by forward addition/backward deletion during PK–PD model optimization. Three random effects for IIV were identified: xenograft size at baseline (BL), growth coefficient (GC) and the Allee effect coefficient (AEC). The resulting overall variability was high due to occasional occurrence of sustained regression in two of the combined treatment groups (Fig. S3). A proportional residual error model was applied to capture the remaining random variability in observed vs. model-fitted xenograft volumes.

The final PK–PD model contained five system-specific fixed effect parameters, two drug-specific and one hybrid parameter (K_{tr}), reflecting both treatment and system-specific properties. Parameters were simultaneously estimated by fitting to xenograft volume measurements over time in all groups. Estimated parameter precision appears adequate, with the highest relative standard error (RSE) on the random effects for IIV. Shrinkage was relatively high (30–40%) for xenograft growth rate and the Allee effect coefficient (Table 3). After PK–PD model optimization, a third and final step was applied to evaluate its ability for a priori forecasting of xenograft growth, inhibition, or regression in other independent studies. The primary focus was to investigate if results from studies with pre-defined, intermittent on/off dosing regimens could be predicted by the model that was developed solely on continuous dosing.

Tumor-bearing mice were dosed for 42 days (1008 h) with either continuous treatment combinations of 75 or 37.5 mg/kg AZD7648 BID plus 100 mg/kg olaparib QD, or various intermittent dosing regimens (Table S1). Sustained regression occurred in individual mice under most intermittent 75 mg/kg QD treatment regimens, but not at a 3 day on/4 day off schedule or at the 37.5 mg/kg AZD7648 dose level. Delayed re-growth was observed in individual mice throughout all seven actively treated groups. Model-forecasts of xenograft regression during treatment generally appear adequate for most of the five intermittently treated groups (Figs. 4 and S8). Only mice under a 3 day on/4 day off schedule at 75 mg/kg AZD7648 BID show re-growth during the final active treatment cycles, a phenomenon not predicted by the model. Post-treatment (> 1008 h) re-growth, or continued regression, is predicted for all groups, with an expected within-group variability increasing after 2–3 treatment weeks, most pronounced in mice dosed at 75 mg/kg AZD7648 BID (Fig. 4). In addition to effect forecasts for intermittent combined exposure, another forecast was performed for continuous 6-week dosage of AZD7648 combined with limited, one-week olaparib dosage. Both observed data and model-predictions show initial tumor shrinkage, followed by delayed regrowth, indicating a lack of sustained effects for the median population prediction, with a high variability in response predicted post-dose (Fig. S9).

Based on the model parameters, tumor static equilibrium (TSE) concentrations were determined for olaparib and AZD7648. These concentrations represent the steady state exposure required to maintain tumor volume at the initial tumor size (Fig. S10, yellow line). Concentration pairings above the TSE represent combinations where tumor regression occurs, while pairings below the TSE are insufficient to drive stasis. Olaparib alone requires a steady-state concentration of 64.9 uM to reach TSE, while AZD7648 is unable to achieve TSE as a monotherapy. In combination, an olaparib concentration of 19.9 uM and an AZD7648 concentration of 20.2 uM is sufficient to reach TSE. The full derivation of the TSE is provided in the supplement.

To better understand why certain schedules achieve greater efficacy, the fractional occupancy of each compartment over time for all treatment groups were simulated (Fig. 5a). All groups achieved apoptotic fractions > 50% during the treatment period. The largest apoptotic fractions were observed in the in 75 mg/kg continuous, 14/14/14, 7/7, and 5/2 (maximum fraction > 70%). These groups also had the largest depletion of proliferating cells (> 90% depletion).

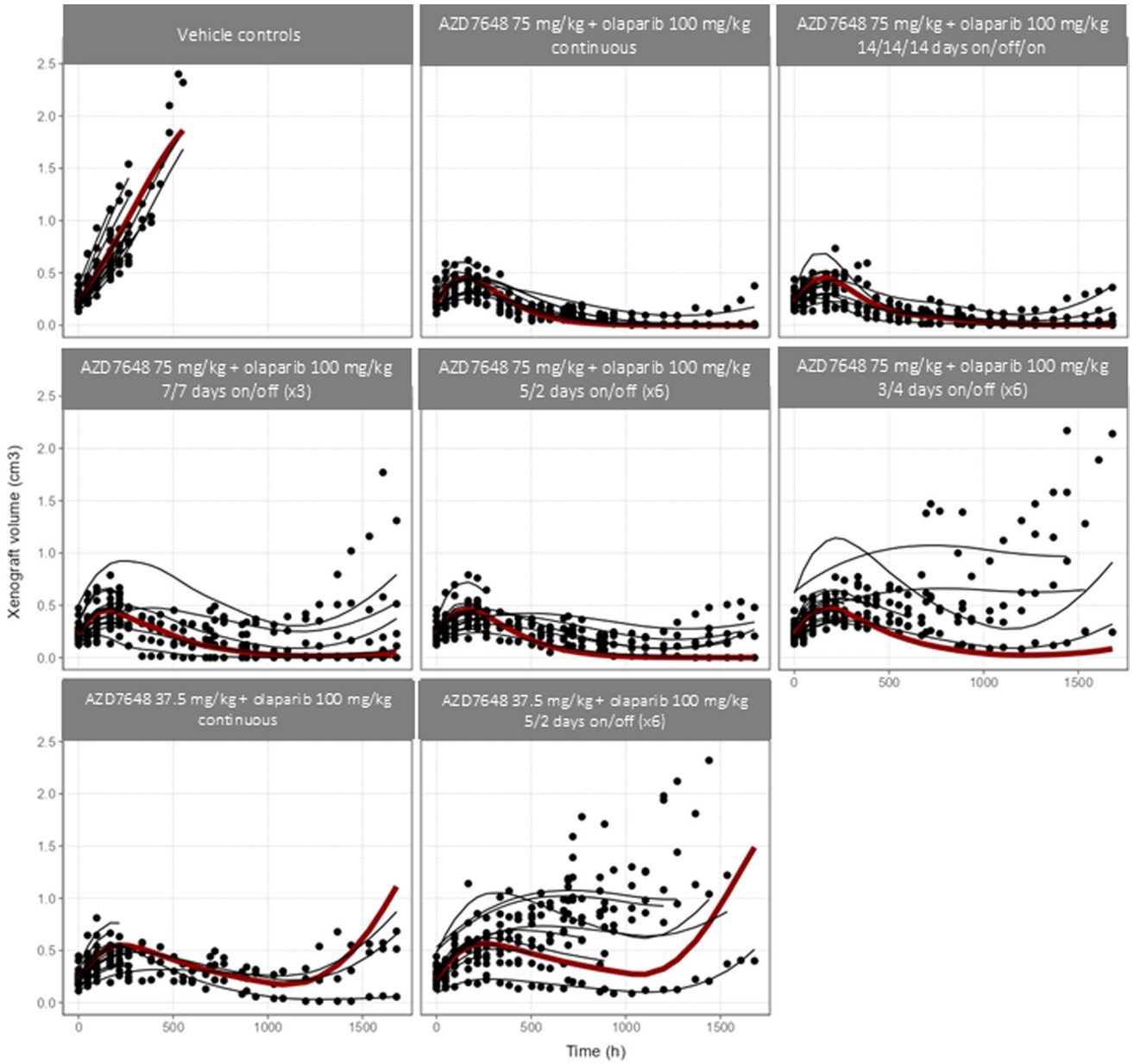

Fig. 4 Model predictions for all treatment groups of 6-week intermittent dosing tumor growth in study S1842 using Allee effect PK–PD model. Individual and mean predictions of AZD7648 + olaparib combinations with different schedules. Filled circles represent individual animal tumor volumes; black lines—individual predictions; red lines—mean predictions. All predictions were made a priori from the finalized PK–PD model (Color figure online)

The 3/4 treatment group reached a similar apoptotic fraction (67%), but did maintain higher levels of the proliferative fraction. Both 37.5 mg/kg groups (continuous, 5/2) sustained an apoptotic fraction < 60%, where limited efficacy was observed.

Additionally, we explored the relationship between efficacy and the fractional population under each treatment condition (Fig. 5b). The fractional population (proliferating, non-proliferating, apoptotic) was quantified using area under the curve during the treatment period. Linear relationships were observed between efficacy, as quantified by fold-change from baseline at the end of dosing, and fractional populations in proliferative ($R^2 = 0.97$) and apoptotic fractions ($R^2 = 0.93$), but not for the quiescent population ($R^2 = 0.42$). The best correlate with efficacy was the ratio of apoptotic:proliferative fractions, suggesting that schedules and doses that deplete the proliferating compartment and drive cells toward apoptosis result in the greatest tumor regressions.

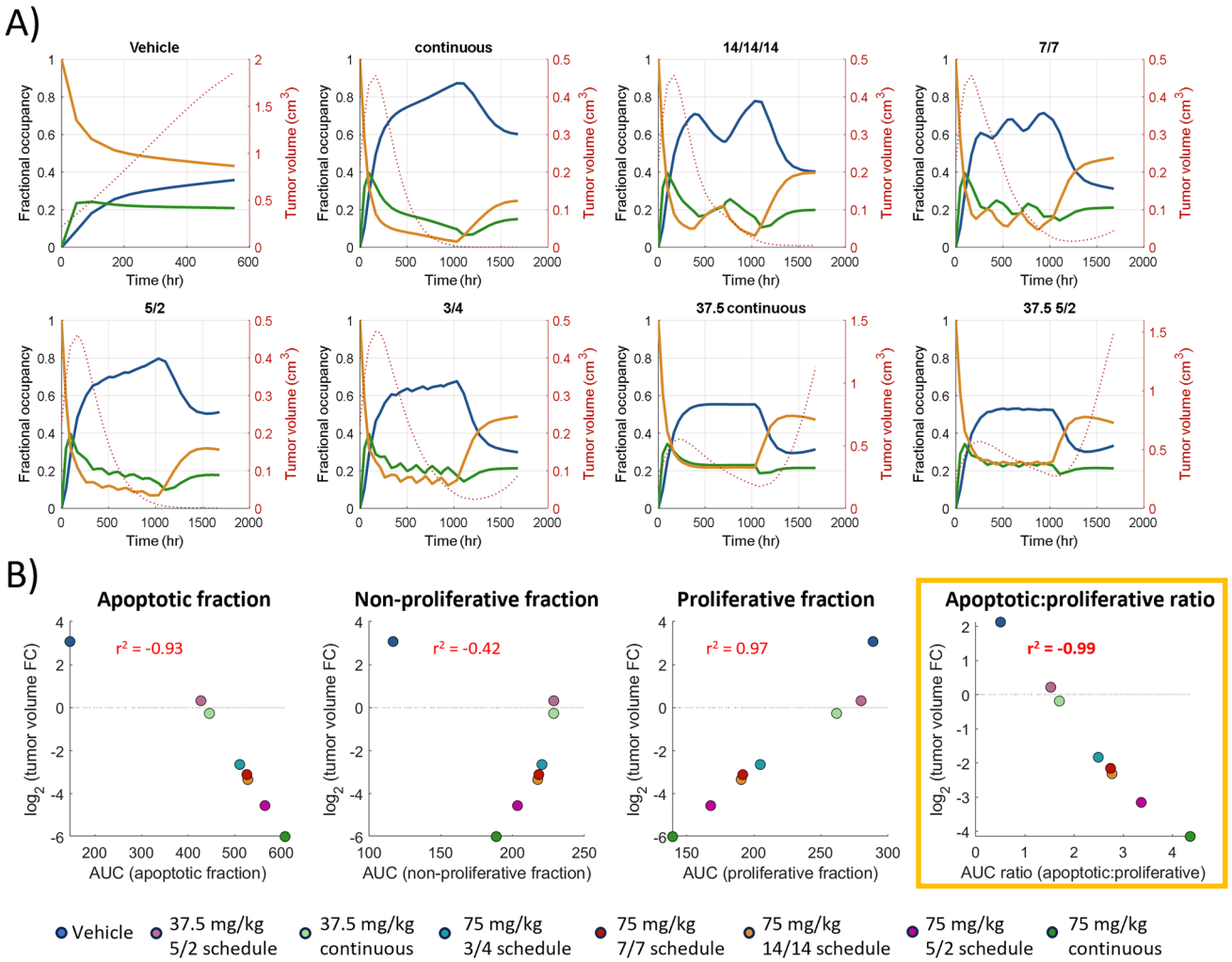

Fig. 5 Model simulations for dose/schedule combinations of AZD7648 + Olaparib. **a** Time course of the fractional occupancy of each compartment from finalized PK–PD model. All treatment groups were simulated with 75 mg/kg or 37.5 mg/kg AZD7648 in combination with 100 mg/kg Olaparib under continuous, 14 on/14 off, 7 on/7 off, 5 on/2 off, or 3 on/4 off schedules. Blue—apoptotic fraction; Green—non-proliferative fraction; Yellow—proliferative fraction. The dashed red line represents the total tumor volume. **b** Correlations of tumor efficacy and fractional occupancies of each compartment. Efficacy was quantified by determining the fold change in tumor volume 24 h after the last dose relative to the baseline volume. Pearson correlation coefficients are shown in red. Dose refers to amount of AZD7648 given twice daily (Color figure online)

Discussion

In pre-clinical oncology studies, pronounced regression resulting from combined drug exposure is frequently labeled in terms of 'synergy' or 'supra-additivity', when compared to the monotherapy activity of individual agents. Various descriptive approaches have been presented, where potency and efficacy are quantified for single agent exposure, with the additional effect for the combination requiring (model-inferred) 'interaction' terms that enhance the monotherapy activity [30–32]. However, this approach does not always explain the observed difference between single and combined treatment at a mechanistic level, nor does it account for non-linear dynamics at low cell densities as expressed by the Allee effect.

The currently presented population PK–PD analysis for effects of various combinations of AZD7648 and olaparib, based on their previously discussed mechanism of action (MoA's) [3], showed an adequate goodness-of-fit for data observed from a study with 28 days of continuous treatment. The Verhulst model was selected from the family of self-limiting growth models [20]. Its limitation term, depending on xenograft size, remains constrained between zero and unity, which makes all other model parameters scalable between various studies. Fitting the Verhulst model to the control data identifies two boundary conditions of the system, i.e. xenograft volume at pre-treatment

baseline (T = 0) specific for each study and the upper equilibrium state of the system, defined by the maximum sustainable size or carrying capacity of the animal for xenografts. The latter condition can never actually be observed (due to ethical reasons), but its value is inferred from the diminished exponential growth occurring at higher volumes. Parameter values of the Verhulst model are drug-independent system parameters, with limited identifiability from unperturbed xenograft growth. They are used as starting values for the next step of the model development.

Dynamic parameters for proliferation, cell state/cycle dynamics and turn-over/apoptosis can only be derived when the system was perturbed by active treatment with olaparib and/or AZD7648. This perturbance is driven by drug-specific MoA's, resulting in dynamic changes from which the underlying parameters can be inferred. Based on the diagnostics from the initial fit of the base model, further iterative model optimization was performed to capture all observed profiles of xenograft growth inhibition, regression and re-growth.

Therefore, various assumptions on the model structure as well as reductions in parameter space must be made to achieve model identifiability and precision under these limitations. For olaparib and AZD7648, exposure to the single compounds at the studied dose levels in S1822 resulted in growth inhibition, but not regression which is only observed in mice exposed to drug combinations at high dose levels. Xenograft regression implies that the rate of cell death exceeds cell proliferation, and the model requires at least one term for removal of cells from the system. This process also occurs in the unperturbed state, but proliferation and background cell death parameters underlying logistic growth in control animals are confounded and cannot be uniquely identified. The current model was defined by proliferating, quiescent and dying cell states with drug effects that perturb the system's equilibrium. Growth inhibition, regression and re-growth can all be described by this system, including observed delays between the start and the end of active treatment and xenograft size.

Results from the PK analysis explain part of the effectiveness of combination treatment from a potential drug-drug interaction (DDI), as AZD7648 exposure results in as an apparent decrease in clearance of olaparib in mice. A dedicated VPC, in which the DDI-term is temporarily removed from the olaparib PK model, demonstrates the magnitude of this effect for multiple dosage (Fig. S2). Fitting the PK–PD model to the observed xenograft data while switching off the DDI effect confirms its relevance, as this results in a highly biased model fit for which individual predictions are not randomly distributed around the population median (Fig. S11). Other goodness-of-fit criteria, such as the MVOF, confirm the relevance of the PK interaction for the PK–PD model.

To describe the sustained regression observed in individual mice, an additional term for inhibited proliferation at low xenograft cell densities is required. In population dynamics, the Allee effect has been studied and reported. It has also been introduced to oncology [26, 29], but, to our knowledge, its potential contribution to treatment efficacy has not been quantified before. Gerlee and coworkers attribute the mechanistic basis of the Alllee effect to disruption of endocrine inter-cell signaling, caused by decreased tumor cell density, that results from treatment [26, 29]. Both weak and strong forms of the Allee effect are described, the latter one relating to tumor shrinkage, as also described by the present analysis. The currently chosen form can, dependent on the treatment schedule, cause a bifurcation ('tipping') point of the system, resulting in either an intermediate equilibrium state, where proliferation exactly equals cell death ('stable disease'), or proceed to complete depletion of the proliferating cell pool if cell death becomes greater than proliferation. In the data set used for model development, this occurs for only two individual mice after combined exposure at high dose levels (Fig. S3). Therefore, inference of model parameters for the Allee effect is associated with substantial uncertainty and related Eta-shrinkage, but is paramount for adequate description (Figs. 3b and S6) as well as prediction (Fig. 4) of individual treatment responses throughout both datasets. This intermediate equilibrium state (TSE) is associated with the tumor static drug concentrations, derived from the model parameters. This is plotted in a nomogram (Fig. S10), derived in supplemental derivation). For the current drug parameters, a minimum olaparib concentration above zero will always be required to achieve TSE. The nomogram suggests that olaparib alone can achieve tumor stasis at steady-state with a concentration of 64.9 uM, while AZD7648 can not. The combination of AZD7648 and olaparib drastically lowers this threshold to achieve stasis, and can achieve combination exposures that drive regression (Fig. S10, upper lines).

Forecasted xenograft dynamics during intermittent AZD7648 treatment regimens mostly showed favorable results (Fig. 4). The poorest prediction was for the 75 mg/kg 3 day on/4 day off schedule where the median treatment efficacy appears slightly overpredicted, as xenografts in some individual mice show re-growth before the end of the 42-day exposure period. Cumulative overall exposure to AZD7648 in this group is lower (43%), relative to groups 2–5 (100–50–72%) based on the 3/7 ratio for active exposure in group 6, while concomitant olaparib exposure in all groups is continuous at 100 mg/kg dose level. Lower exposure levels could potentially induce one or more bio-chemical escape mechanisms that would result in development of tolerance to treatment over time, which has been modeled previously for EGFR inhibitors and chemotherapies [33, 34]. However, no indications for such phenomena appear from

GoF diagnostics of the final model fit for 28-day continuous treatment in S1822 at the lowest AZD dose level of 50 mg/kg in group 5 or 6 (Figs. S6 and S7).

The model was used to explore the simulated fractional occupancy in each compartment to understand determinants that lead to optimal efficacy for various schedules. The most effective combination treatment was continuous dosing of AZD7648 and olaparib, but several other treatment schedules were predicted to achieve similar levels of tumor regression. The extent of tumor efficacy was correlated to both the overall reduction in proliferative cells and increase in production of apoptotic cells. Although either of these criteria are suitable, there is the possibility of certain dosing schedules where either event is not sufficient to drive regression. Interestingly, the model suggests that intermittent dosing can sustain regressions as long as the combined dosing period overlaps for a substantial period (> 3 days). While there does seem to be a threshold of dying cells required to achieve tumor regression, the dying population can decrease for a significant amount of time as observed in the 14/14/14 and 7/7 schedules. However, shorter periods of AZD7648 holiday (3 days on/4 days off) are predicted to have worse efficacy if the dosing period does not overlap for a sufficient period.

Previously, an independent study in the same mice strain (not included in current model analysis), under 42 days of intermittent AZD7648 treatment, reported earlier that 7 day on/14 day off and 7 day on/21 day off schedules did show tolerance development, starting approximately 28 days after study start, but the 7 day on/7 day off and 14 day on/14 day off schedules in the same study did not [3]. As Olaparib was continuously dosed during the entire 42-day treatment period, these results suggested that potential tolerance development may occur to effects of AZD7648 and may be related to the time on- and off-treatment.

Other possible causes for apparent changes in treatment efficacy over time may be related to changes in the DDI between AZD7648 and olaparib at the PK level [35]. DDI is implemented in the PK model underlying the current PK–PD analysis (Table 2), but the observed plasma data on this were limited to a 7-day exposure period from the PK studies. In addition, drug concentrations in the xenograft itself were not measured. Furthermore, dose ranges were constrained to 50–100 mg/kg/day for each compound, with only a single dose level for mono-exposure observed for each drug. Such study design may cause a certain degree of confounding between drug-effect parameters for AZD7648 and olaparib that are simultaneously estimated from the PK–PD model fit.

In addition, the selective, non-random drop-out of individual mice over time may contribute to perceived discrepancies between reported and forecasted median xenograft data (Figs. 4 and S12). Removal of animals expressing a relatively favorable efficacy may be associated with dose-limiting toxicity and an apparent overprediction of efficacy may result from this, as animals remaining in such treatment groups are expressing less efficacious responses relative to the median. It can be concluded that discrepancies between the model-forecasted efficacy and observed xenograft profiles in S1842 can be explained by a combination of factors that are partly biological (tolerance development) and partly related to study design limitations (right-hand censoring of individuals with high treatment efficacy combined with MTD-related BW loss).

The interaction at the effect level appearing from the observations as well as from the model analysis, resulting from combination treatment, can be abstracted by the Area Between Effect Curve and baseline (ABEC) introduced by Earp and coworkers in 2004 [36]. Based on this concept, it can be concluded that the cumulative tumor burden under combination treatment at the highest dose levels demonstrates a supra-additive response compared to the respective mono-treatment groups (Fig. S13). This is the result of the dedicated mechanism of action for each drug in the xenograft growth and regression PK–PD model at the proliferative and quiescent compartments respectively.

In summary, xenograft growth, inhibition and regression observed in animals exposed to AZD7648 and/or olaparib, was described and forecasted by a semi-mechanistic model that incorporated the MoA of the respective drugs, that links to proliferative, quiescent, and cell death states. Due to study design limitations, certain assumptions were made on the structure of the xenograft system, which were partly based on the literature and partly on various GoF criteria. In addition, parameter space reduction(s) were performed to ensure PK–PD model identification and parameter precision. Evaluation of model forecasts from xenograft profiles obtained from other studies indicated the possibility of drug tolerance to treatment over time, but additional explanations cannot be excluded due to study and data limitations.

Conclusion

In the present approach, gradual and temporary inhibition of xenograft growth under mono-treatment and the substantial, and sometimes permanent, regression observed from combined exposure was successfully described and predicted from a single parsimonious model structure, reflecting key pathways between cell states and perturbation according to specific MoA's. Based on the current model and underlying assumptions, the aggregate effects of combination treatment can be analyzed from both compound's specific mechanisms of action. This type of model incorporates the individual mechanistic features of the monotherapies, with a structure that remains simple enough that it is identifiable. Such a model is advantageous to explore the full dose/exposure

range of the combination when it is not feasible to experimentally test each possible combination. Furthermore, the model can be utilized to assess what exposures would be necessary in the clinic by linking it to observed or predicted human PK exposures.

Supplementary Information The online version contains supplementary material available at https://doi.org/10.1007/s10928-025-09962-x.

Acknowledgements All funding for this research was provided by AstraZeneca The authors would like to thank Dr. Martijn van Noort (LAP&P consultants) for contribution by deriving the tumor static concentration function and the resulting nomogram for drug combinations.

Author contributions J.DJ and R.R wrote the manuscript. A.R-M and A.S conducted most of the experiments. Model building and validation was performed by J.DJ and T.vS. Data analysis was performed by J.DJ and R.R. M.D, J.DJ, E.C, R.R and T.vS were responsible for conception and oversight of the project.

Funding All funding for this research was provided by AstraZeneca.

Data availability Model code and simulation results are provided in the supplemental material.

Declarations

Conflict of interest E.C, M.D, A.R-M, A.S, R.R are employees of AstraZeneca and hold stock in the company.

References

1. Alkan O, Schoeberl B, Shah M, Koshkaryev A, Heinemann T, Drummond DC et al (2018) Modeling chemotherapy-induced stress to identify rational combination therapies in the DNA damage response pathway. Sci Signal 11(540)
2. Checkley S, MacCallum L, Yates J, Jasper P, Luo H, Tolsma J et al (2015) Bridging the gap between in vitro and in vivo: dose and schedule predictions for the ATR inhibitor AZD6738. Sci Rep 5:13545
3. Fok JHL, Ramos-Montoya A, Vazquez-Chantada M, Wijnhoven PWG, Follia V, James N et al (2019) AZD7648 is a potent and selective DNA-PK inhibitor that enhances radiation, chemotherapy and olaparib activity. Nat Commun 10(1):5065
4. Fong PC, Boss DS, Yap TA, Tutt A, Wu P, Mergui-Roelvink M et al (2009) Inhibition of poly(ADP-ribose) polymerase in tumors from BRCA mutation carriers. N Engl J Med 361(2):123–134
5. Hodgson DR, Dougherty BA, Lai Z, Fielding A, Grinsted L, Spencer S et al (2018) Candidate biomarkers of PARP inhibitor sensitivity in ovarian cancer beyond the BRCA genes. Br J Cancer 119(11):1401–1409
6. Saad F, Clarke NW, Oya M, Shore N, Procopio G, Guedes JD et al (2023) Olaparib plus abiraterone versus placebo plus abiraterone in metastatic castration-resistant prostate cancer (PROpel): final prespecified overall survival results of a randomised, double-blind, phase 3 trial. Lancet Oncol 24(10):1094–1108
7. Kindler HL, Hammel P, Reni M, Van Cutsem E, Macarulla T, Hall MJ et al (2022) Overall survival results from the POLO trial: a phase III study of active maintenance olaparib versus placebo for germline BRCA-mutated metastatic pancreatic cancer. J Clin Oncol 40(34):3929–3939
8. Pommier Y, O'Connor MJ, de Bono J (2016) Laying a trap to kill cancer cells: PARP inhibitors and their mechanisms of action. Sci Transl Med 8(362):362ps17
9. Balmus G, Pilger D, Coates J, Demir M, Sczaniecka-Clift M, Barros AC et al (2019) ATM orchestrates the DNA-damage response to counter toxic non-homologous end-joining at broken replication forks. Nat Commun 10(1):87
10. Cardilin T, Almquist J, Jirstrand M, Gabrielsson J (2018) Evaluation and translation of combination therapies in oncology—a quantitative approach. Eur J Pharmacol 834:327–336
11. Tate SC, Burke TF, Hartman D, Kulanthaivel P, Beckmann RP, Cronier DM (2016) Optimising the combination dosing strategy of abemaciclib and vemurafenib in BRAF-mutated melanoma xenograft tumours. Br J Cancer 114(6):669–679
12. Jones RDO, Petersson K, Tabatabai A, Bao L, Tomkinson H, Schuller AG (2023) Pharmacokinetic/pharmacodynamic analysis of savolitinib plus osimertinib in an EGFR mutation-positive, MET-amplified non-small cell lung cancer model. Mol Cancer Ther 22(5):679–690
13. Yates JW, Ashton S, Cross D, Mellor MJ, Powell SJ, Ballard P (2016) Irreversible inhibition of EGFR: modeling the combined pharmacokinetic–pharmacodynamic relationship of osimertinib and its active metabolite AZ5104. Mol Cancer Ther 15(10):2378–2387
14. Bauer RJ (2019) NONMEM tutorial Part I: description of commands and options, with simple examples of population analysis. CPT Pharmacometrics Syst Pharmacol 8(8):525–537
15. Bauer RJ (2019) NONMEM tutorial Part II: estimation methods and advanced examples. CPT Pharmacometrics Syst Pharmacol 8(8):538–556
16. Mould DR, Upton RN (2013) Basic concepts in population modeling, simulation, and model-based drug development-part 2: introduction to pharmacokinetic modeling methods. CPT Pharmacometrics Syst Pharmacol 2(4):e38
17. Upton RN, Mould DR (2014) Basic concepts in population modeling, simulation, and model-based drug development: part 3-introduction to pharmacodynamic modeling methods. CPT Pharmacometrics Syst Pharmacol 3(1):e88
18. Nguyen TH, Mouksassi MS, Holford N, Al-Huniti N, Freedman I, Hooker AC et al (2017) Model evaluation of continuous data pharmacometric models: metrics and graphics. CPT Pharmacometrics Syst Pharmacol 6(2):87–109
19. Savic RM, Karlsson MO (2009) Importance of shrinkage in empirical bayes estimates for diagnostics: problems and solutions. AAPS J 11(3):558–569
20. Sharma A, Jusko WJ (1998) Characteristics of indirect pharmacodynamic models and applications to clinical drug responses. Br J Clin Pharmacol 45(3):229–239

21. Mould DR, Walz AC, Lave T, Gibbs JP, Frame B (2015) Developing exposure/response models for anticancer drug treatment: special considerations. CPT Pharmacometrics Syst Pharmacol 4(1):e00016
22. Lobo ED, Balthasar JP (2002) Pharmacodynamic modeling of chemotherapeutic effects: application of a transit compartment model to characterize methotrexate effects in vitro. AAPS PharmSci 4(4):E42
23. Krzyzanski W (2011) Interpretation of transit compartments pharmacodynamic models as lifespan based indirect response models. J Pharmacokinet Pharmacodyn 38(2):179–204
24. Simeoni M, Magni P, Cammia C, De Nicolao G, Croci V, Pesenti E et al (2004) Predictive pharmacokinetic–pharmacodynamic modeling of tumor growth kinetics in xenograft models after administration of anticancer agents. Cancer Res 64(3):1094–1101
25. Allee WC (1926) Studies in animal aggregations: Causes and effects of bunching in land isopods. J Exp Zool 45(1):255–277
26. Neufeld Z, von Witt W, Lakatos D, Wang J, Hegedus B, Czirok A (2017) The role of Allee effect in modelling post resection recurrence of glioblastoma. PLoS Comput Biol 13(11):e1005818
27. Delitala M, Ferraro M (2020) Is the Allee effect relevant in cancer evolution and therapy? AIMS Mathematics
28. Fadai NT, Simpson MJ (2020) Population dynamics with threshold effects give rise to a diverse family of Allee effects. Bull Math Biol 82(6):74
29. Gerlee P, Altrock PM, Malik A, Krona C, Nelander S (2022) Autocrine signaling can explain the emergence of Allee effects in cancer cell populations. PLoS Comput Biol 18(3):e1009844
30. Miao X, Koch G, Straubinger RM, Jusko WJ (2016) Pharmacodynamic modeling of combined chemotherapeutic effects predicts synergistic activity of gemcitabine and trabectedin in pancreatic cancer cells. Cancer Chemother Pharmacol 77(1):181–193
31. Terranova N, Germani M, Del Bene F, Magni P (2013) A predictive pharmacokinetic–pharmacodynamic model of tumor growth kinetics in xenograft mice after administration of anticancer agents given in combination. Cancer Chemother Pharmacol 72(2):471–482
32. Wilson S, Tod M, Ouerdani A, Emde A, Yarden Y, Adda Berkane A et al (2015) Modeling and predicting optimal treatment scheduling between the antiangiogenic drug sunitinib and irinotecan in preclinical settings. CPT Pharmacometrics Syst Pharmacol 4(12):720–727
33. Claret L, Girard P, Hoff PM, Van Cutsem E, Zuideveld KP, Jorga K et al (2009) Model-based prediction of phase III overall survival in colorectal cancer on the basis of phase II tumor dynamics. J Clin Oncol 27(25):4103–4108
34. Eigenmann MJ, Frances N, Lave T, Walz AC (2017) PKPD modeling of acquired resistance to anti-cancer drug treatment. J Pharmacokinet Pharmacodyn 44(6):617–630
35. McCormick A, Swaisland H, Reddy VP, Learoyd M, Scarfe G (2018) In vitro evaluation of the inhibition and induction potential of olaparib, a potent poly(ADP-ribose) polymerase inhibitor, on cytochrome P450. Xenobiotica 48(6):555–564
36. Earp J, Krzyzanski W, Chakraborty A, Zamacona MK, Jusko WJ (2004) Assessment of drug interactions relevant to pharmacodynamic indirect response models. J Pharmacokinet Pharmacodyn 31(5):345–380